IEEE Access
Multidisciplinary ⋮ Rapid Review ⋮ Open Access Journal

Received 18 June 2024, accepted 1 July 2024, date of publication 10 July 2024, date of current version 29 July 2024.

Digital Object Identifier 10.1109/ACCESS.2024.3426051

RESEARCH ARTICLE

Resistors and Capacitors in Series Mid-Point Grounding for Protection Application in Unipolar Low Voltage DC System

SEUNG-TAEK LIM[1], KI-YEON LEE[1], DONG-JU CHAE[1], CHAN-HYEOK OH[1], AND SUNG-HUN LIM[2]

[1]Electrical Safety Research Institute, Korea Electrical Safety Corporation, Wanju 55365, South Korea
[2]Department of Electrical Engineering, Soongsil University, Seoul 06978, South Korea

Corresponding author: Sung-Hun Lim (superlsh73@ssu.ac.kr)

This work was supported by the Energy Efficiency and Resources of Korea Institute of Energy Technology Evaluation and Planning (KETEP) grant funded by Korean Government Ministry of Trade, Industry, and Energy under Grant RS-2024-00421164.

ABSTRACT With climate anomalies and ecosystem destruction caused by global warming, reducing carbon emissions is becoming increasingly important. Consequently, the power industry is investing in new sectors such as expanding renewable energy and utilizing DC grids to enhance energy efficiency and reduce coal fuel usage. The use of DC systems for carbon emission reduction is expected, and low-voltage direct current (LVDC) systems are continuously being investigated as efficient power systems. Existing studies have primarily focused on power conversion design and operation, but studies on the protection system configuration for the electrical safety of end users are insufficient. Therefore, this study analyzes the characteristics of resistors and capacitors in series (RCS) mid-point grounding in uni-polar LVDC systems for use at the end of LVDC systems and reviews protection systems against electrical shock and ground faults using DC residual current devices (DC–RCDs) and insulation monitoring devices (IMDs). Through fault tests, the appropriateness of using the protection system with these devices in RCS mid-point grounding configurations is verified. The fault test demonstrated that the RCS mid-point grounding LVDC system could detect and protect against faults within 80 ms using a DC-RCD. Additionally, it was confirmed that faults could be detected and cleared within 4 min using an IMD in the event of a high-resistance fault, enabling the use of IMD which was not feasible in grounding systems. Our research results contribute to the use of LVDC systems by establishing a protection system based on relatively inexpensive mechanical circuit breakers instead of high-cost semiconductor-based breakers often mentioned for consumer protection devices.

INDEX TERMS DC-RCD, electrical safety, electrical shock, IMD, LVDC, mid-point.

I. INTRODUCTION

The average temperature of the Earth is continuously rising due to accelerating global warming. To address this problem, extensive international efforts are underway to reduce greenhouse gases and carbon emissions [1], [2]. In response, the energy industry is striving to change the electrical energy environment by increasing the use of renewable energy and employing high-efficiency energy devices to reduce power losses [3], [4]. Due to lower line losses compared to AC power systems, DC power systems can reduce power conversion losses caused by AC–DC power conversion. The use of DC systems is expected to increase with the expansion of DC equipment such as electric vehicle charging facilities and solar power generation [5], [6].

Globally, markets related to DC distribution are expected to grow by 7.04% annually due to the expansion of DC equipment in household appliances, Internet data centers,

The associate editor coordinating the review of this manuscript and approving it for publication was Yonghao Gui.

© 2024 The Authors. This work is licensed under a Creative Commons Attribution-NonCommercial-NoDerivatives 4.0 License.
For more information, see https://creativecommons.org/licenses/by-nc-nd/4.0/

and electric vehicle charging facilities [7]. In households, most appliances such as light-emitting diodes (LEDs), televisions (TVs), and computers ultimately use DC power, and the use of DC distribution can reduce losses that occur during AC–DC power conversion [8].

Within households, low-voltage direct current (LVDC) systems are becoming more accessible to both industry professionals and ordinary electrical users, increasing the risk of safety accidents. However, no specific domestic or international standards or guidelines for the safety of LVDC systems have been established [9], [10], [11]. Therefore, electrical safety is a critical factor in residential LVDC systems that are close to the end user, and safety analysis is essential [12], [13], [14], [15], [16].

Recently, with the development of power semiconductors and high-frequency transformers, the use of LVDC systems is expected to continuously increase. Several studies are being conducted to improve efficiency in consumer facilities. Compared to AC power systems, DC power systems can improve energy efficiency, enhance power quality, and reduce construction costs, resulting in an efficiency increase of more than 5% for loads [17], [18]. Unlike AC systems, DC systems have different fault characteristics based on the grounding configuration due to the presence of polarity and frequency [19], [20].

In particular, DC systems have an extremely impulsive short fault current and a different characteristic of electric shock compared to AC systems [21], [22], [23]. Consequently, some studies on DC grounding systems and electrical shock have been conducted. In [24], operating time of the DC-RCD was proposed to be within 10 ms, considering electrical shock and DC grounding systems. In [25] and [26], solid-state circuit breaker (SSCB) has been proposed to prevent ventricular fibrillation. However, SSCBs are currently expensive and difficult to apply in practical applications, necessitating an alternative solution. Although some studies have highlighted the need for protection against DC leakage, reflecting human resistance and ventricular fibrillation, practical application from the consumer's perspective remains challenging [27], [28], [29].

Therefore, this paper proposes a grounding configuration using a DC-RCD with practical specifications to protect against electric shock and ground faults. It also aims to enhance safety in LVDC systems by incorporating a secondary protection system with insulation monitoring devices (IMDs).

II. CHARACTERISTICS OF GROUNDING CONFIGURATION IN LVDC

IEC 60364-1 classifies power systems based on the grounding configuration at the source and the protective earth (PE) grounding in the distribution line [30]. According to this standard, systems are typically classified into three types: TT, IT, and TN systems. The presence of polarity in DC systems allows for a greater variety of configurations than AC systems, each configuration has different characteristics.

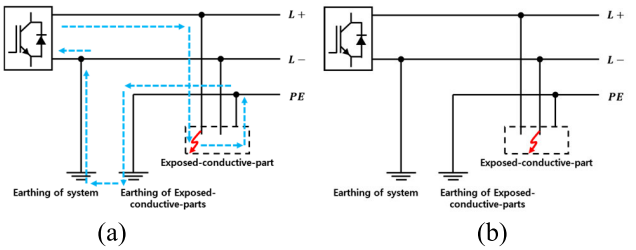

FIGURE 1. Example of the fault current path according to fault polarity in TT grounding system (a) different-polarity fault (b) same-polarity fault.

A. PROTECTIVE DEVICE CONFIGURATION ACCORDING TO GROUNDING

Each grounding system has distinct fault characteristics, requiring specific protective devices. In IT systems, RCDs cannot be used because no fault current flows during a primary fault, whereas TT and TN grounding systems can use RCDs. However, as shown in Fig. 1, protection against same-polarity faults, which occur at the same pole as the system ground, cannot be achieved. Secondary faults can lead to overcurrent and equipment failure, and in DC systems, electrolytic corrosion can also cause structural damage. Therefore, early detection and protection are required.

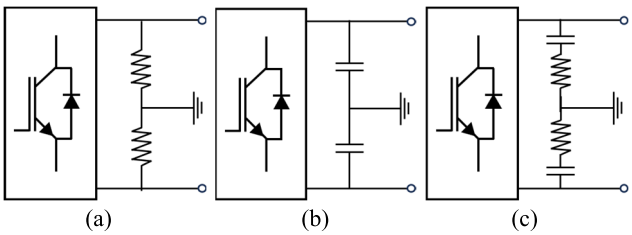

FIGURE 2. Configuration of the mid-point grounding (a) with resistors (b) with capacitors (c) with resistors and capacitors.

B. MID-POINT GROUNDING SYSTEM

The mid-point grounding configuration can be achieved using passive components such as resistors, capacitors, and diodes [16]. As depicted in Fig. 2(a), resistor mid-point grounding reduces the voltage between the power line and ground to half the operating voltage, improving safety and enabling protection through RCDs. However, depending on the resistor value, the fault current may be small, requiring high-performance sensors, and the use of IMDs is not possible. Additionally, continuous losses occur under normal conditions due to the resistor mid-point grounding current. Losses in the normal state can be reduced by using capacitors for mid-point grounding, as shown in Fig. 2(b). However, impulsive high fault currents can occur in case of short circuits or ground faults, posing risks to equipment and human safety. Additionally, short impulsive fault currents are difficult to detect, limiting the use of current-based protective devices. Furthermore, an effect similar to increased line capacitance leads to long detection times for an IMD, making the protective device cannot easily be used. In this paper proposes an RCS mid-point grounding configuration

TABLE 1. Characteristic of Mid-point grounding Configuration according to the elements.

	Resistor	Capacitor	Resistor + Capacitor
Power loss in normal state	Occurs	Does not occur	Does not occur
Short circuit current	Normal short circuit current	Impulsive high current occurs	Limited impulsive short circuit current occurs
Inrush current	Low	Very high	Can be limited
RCD application	Possible	Difficult	Possible
IMD application (Detect high resistance fault)	Impossible	Difficult	Possible

with resistors and capacitors in series, as shown in Fig. 2(c), to prevent normal state losses and limit impulsive fault current. The characteristics of each mid-point grounding configuration are presented in Table 1. Along with these characteristics, the operation of protective devices in LVDC with the RCS mid-point grounding configuration was analyzed for electrical safety.

III. CHARACTERISTICS OF HUMAN ELECTRIC SHOCK BY DC SOURCE

Fig. 3 shows a graph from IEC 60479 illustrating the patho-physiological effects on the human body relative to the duration of DC current flow, specifically for a path from the feet to the left hand. Detailed effects on the human body for each zone (DC-1 to DC-4) are presented in Table 2.

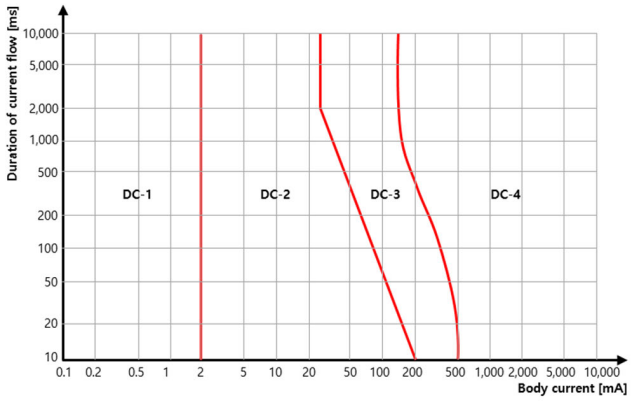

FIGURE 3. Graph illustrating the time/current zones of effects of DC flow on the human body for a longitudinal upward current path (feet to left hand).

Table 3 presents the internal body resistance ratio and heart current factor (F) for each path from the left hand to the foot. The heart current factor calculates the risk of ventricular fibrillation for electric shock along each path as a body current from electric shock from the left hand to both feet, as expressed in Eq. (1) [18].

$$I_h = \frac{I_{ref}}{F} \tag{1}$$

I_h : Body current for each electric shock path in Table 3

TABLE 2. Physiological effects for DC flow in IEC 60479.

Zone	Physiological effects
DC-1	Slight pricking sensation is possible when making, breaking, or rapidly altering current flow.
DC-2	Involuntary muscular contractions are likely, especially when making, breaking, or rapidly altering current flow, but usually no harmful electrical physiological effects.
DC-3	Strong involuntary muscular reactions and reversible disturbances of formation and conduction of impulses in the heart may occur, increasing with the current magnitude and time. Generally, no organic damage is expected.
DC-4	Pathophysiological effects may occur such as cardiac arrest, breathing arrest, burns, or other cellular damage. Probability of ventricular fibrillation increases with current magnitude and time.

TABLE 3. Internal boby resistance depending on current path.

No.	current Path	Body resistance ratio [%]	Heart Current Factor(F)
1	Left hand to left foot or right foot	100	1
2	Left hand to both feet	74.25	1
3	Both hands to both feet	50.65	1
4	Left hand to right hand	80.7	0.4
5	Right hand to left foot or right foot	100	0.8
6	Right hand to both feet	74.25	0.8
7	Back to right hand	48.1	0.3
8	Back to left hand	48.1	0.7
9	Chest to right hand	52.4	1.3
10	Chest to left hand	52.4	1.5
11	Seat to left hand or right hand	56.5	0.7
12	Seat to both hands	32.9	0.7
13	Left foot to right foot	101.5	0.04

I_{ref} : Body current for electric shock from left hand to both feet

F : Heart current factor

The body resistance and the body current causing ventricular fibrillation, applied to the body current path, are used to select the parameters of the RCS mid-point grounding to minimize the electric shock hazard.

IV. RCS MID-POINT GROUNDING CONFIGURATION AND PROTECTION SYSTEM PROPOSAL

A. RCS MID-POINT GROUNDING CONFIGURATION

Since the RCS mid-point grounding configuration comprises resistors and capacitors, as shown in Fig. 2(c) [31], it limits the impulsive fault current in the event of a fault. The impulsive fault current and the peak current during a fault can be expressed in Eqs. (2) and (3), respectively.

$$i_F = I_{CP} \cdot e^{-\frac{t}{R_{CBr} \cdot Cm}} \tag{2}$$

$$I_{CP} = \frac{E_C}{R_{CBr}} \tag{3}$$

where I_{CP} represents the peak value of the impulsive fault current, E_C denotes the pre-fault voltage across the capacitor, R_{CBr} denotes the equivalent resistance inside and outside

the capacitor, and C_m denotes the capacitance value of the mid-point grounding configuration.

By selecting appropriate parameters for the capacitor and resistor, a system that enables current-based protection and high-resistance fault detection using an IMD can be configured.

B. INRUSH CURRENT ANALYSIS OF THE RCS MID-POINT GROUNDING CONFIGURATION

In DC systems, the inrush current induced by capacitors during initial power application can trigger protective devices and potentially damage auxiliary equipment. Therefore, the inrush current of the RCS mid-point grounding configuration was analyzed.

Eq. (4) represent the inrush current (i_{inrush}) generated by the RCS mid-point when power is applied, and Eq. (5) represents the peak of the inrush current (I_{inrush}), where R_m denotes the resistive component of the mid-point, and R_{inrush} and C_{inrush} represent the equivalent resistance and capacitor of the RCS mid-point.

$$i_{inrush}(t) = I_{inrush} e^{-\frac{t}{R_{inrush} C_{inrush}}} \tag{4}$$

$$I_{inrush} = \frac{U}{R_{inrush}} = \frac{U}{2R_m} \tag{5}$$

Hence, the magnitude of the inrush current in the RCS mid-point grounding configuration is influenced by the voltage applied to the mid-point (U) and the mid-point resistance (R_m), indicating that the inrush current can be controlled through parameter selection. Typically, the output of converters exhibits a ramp shape; therefore, the inrush current should not exceed the maximum inrush current.

C. RCS MID-POINT GROUNDING CONFIGURATION PARAMETER SELECTION

In the RCS mid-point grounding configuration, the resistor serves to constrain the impulsive current caused by the capacitor during a fault, thereby diminishing the likelihood of ventricular fibrillation in humans. Consequently, when selecting the resistor parameters, careful consideration was given to the impulsive discharge characteristics of the fault current and the electrical path of human electric shock. The current capable of inducing ventricular fibrillation in humans, as per IEC 60479, is 140 mA, thus, for safety, a ventricular fibrillation safe current (I_{h_RMS}) of 100 mA was chosen. According to IEC 60479-2, the peak value (I_{h_P}) of the impulsive current caused by a capacitor with an RMS value of 100 mA is represented as $\sqrt{6}$times the RMS value of the impulsive current. Similarly, the ventricular fibrillation risk current (I_P) considering the electric shock path can be determined. The electric shock current for each path can be computed using Eq. (6), taking into account the human body resistance (R_{body}) and the ventricular fibrillation risk current. Herein, the human body resistance is based on 700 Ω from the left hand to the right hand, and the resistance values for each path are derived and presented in Table 4.

$$R_m = \frac{U}{I_P} - R_{body} \tag{6}$$

In this study, to mitigate the likelihood of ventricular fibrillation across all paths, the highest derived resistance value, 1872 Ω for path 10 (chest to left hand), was selected as the resistance value for the RCS mid-point grounding configuration.

TABLE 4. Characteristic of Mid-point grounding Configuration.

	I_{h_P} [mA]	F	I_P [mA]	R_b[Ω]	R_m[Ω]
1	244.95	1	244.95	867.41	683.93
2	244.95	1	244.95	644.05	907.29
3	244.95	1	244.95	439.34	1112.00
4	244.95	0.4	612.37	700.00	-79.46
5	244.95	0.8	306.19	867.41	373.66
6	244.95	0.8	306.19	644.05	597.02
7	244.95	0.3	816.50	417.22	48.18
8	244.95	0.7	349.93	417.22	668.72
9	244.95	1.3	188.42	454.52	1562.22
10	244.95	1.5	163.30	454.52	1872.49
11	244.95	0.7	349.93	490.09	595.85
12	244.95	0.7	349.93	285.38	800.56
13	244.95	0.04	6123.72	880.42	-818.37

Generally, RCD operation occurs when the fault current exceeds the rated residual current and persists for a specific duration. Consequently, if this duration is not met, the RCD will not operate. In the RCS mid-point grounding configuration, for a DC-RCD to operate properly, the discharge current from the capacitor must exceed the rated residual current for a period longer than the operating time of the DC-RCD. Hence, the capacitance required can be determined using Eq. (7).

$$C_m = \frac{t}{R_{CBr} \times \{ln(I_{CP}) - ln(i_F(t))\}} \tag{7}$$

Given the absence of readily available DC-RCDs, a cut-off time of 0.1 s and a rated residual current of 80 mA were employed to select the capacitor value for the RCS mid-point grounding configuration, following IEC 63053 guidelines concerning residual current operated protective devices for DC systems. The capacitors should sustain the residual current above 80 mA for 0.1 s after capacitor discharge across all electrical shock paths, as detailed in Table 5. Consequently, to ensure the fault current's operating time, a capacitance value of approximately 66 μF from path 13 (left foot to right foot) is chosen for the RCS mid-point grounding structure.

D. EXAMINATION OF IMD USAGE IN RCS MID-POINT GROUNDING CONFIGURATION

IMDs primarily measure the insulation resistance value in parallel to the line. Detection time lengthens with increased line capacitance. When the RCS mid-point is applied, it operates as shown in Fig. 4(a), but from the perspective of IMDs, it functions as shown in Fig. 4(b). Here, R_{m_eq} and C_{m_eq} indicate the equivalent resistances of R_m and C_m in Fig. 4(a). Therefore, R_{m_eq} affects the IMD's measurement value, while C_{m_eq} influences the detection speed.

TABLE 5. Characteristic of Mid-point grounding Configuration.

	E_C [V]	R_m [Ω]	R_b [Ω]	I_P [mA]	$i_F(0.1)$ [mA]	C_m [μF]
1	380	1872.49	867.41	138.69	0.08	66.33
2	380	1872.49	644.05	151.00	0.08	62.55
3	380	1872.49	439.34	164.37	0.08	60.07
4	380	1872.49	700.00	147.72	0.08	63.39
5	380	1872.49	867.41	138.69	0.08	66.33
6	380	1872.49	644.05	151.00	0.08	62.55
7	380	1872.49	417.22	165.96	0.08	59.85
8	380	1872.49	417.22	165.96	0.08	59.85
9	380	1872.49	454.52	163.30	0.08	60.22
10	380	1872.49	454.52	163.30	0.08	60.22
11	380	1872.49	490.09	160.84	0.08	60.61
12	380	1872.49	285.38	176.10	0.08	58.73
13	380	1872.49	880.42	138.04	0.08	66.59

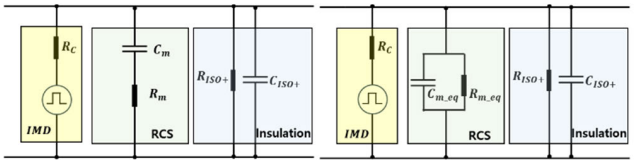

(a) basic circuit (b) equivalent circuit

FIGURE 4. Simplified IMD application circuit.

Through the equivalent circuit shown in Fig. 4(b), resistance Eq. (8) and capacitance Eq. (9) for the RCS mid-point grounding configuration can be derived.

$$\boldsymbol{R_{m\_eq}} = \left\{1 + \left(\omega \boldsymbol{R_{m\_eq}} \boldsymbol{C_{m\_eq}}\right)^2\right\} \boldsymbol{R_m} \tag{8}$$

$$\boldsymbol{C_{m\_eq}} = \boldsymbol{C_m}\left[1 + \left(\frac{1}{\omega \boldsymbol{R_{m\_eq}} \boldsymbol{C_{m\_eq}}}\right)^2\right]^{-1} \tag{9}$$

$\boldsymbol{R_{m\_eq}}$ increases in comparison to $\boldsymbol{R_m}$, whereas $\boldsymbol{C_{m\_eq}}$ decreases relative to $\boldsymbol{C_m}$, signifying a reduction in the impact on IMD measurements attributable to the RCS mid-point grounding configuration.

E. CONFIGURATION OF PROTECTION SYSTEM IN RCS MID-POINT GROUNDING

In contrast to resistor or capacitor mid-point grounding configurations, the RCS mid-point grounding configuration allows for the utilization of IMD and suggests a secondary protection method using IMDs, as depicted in Fig. 5. Protection against faults exceeding the rated residual current resulting from ground faults or electric shocks is achievable with DC-RCD. In instances where DC-RCD does not operate, fault detection by IMDs and power disconnection by interconnected DC-RCDs can prevent secondary faults.

V. VERIFICATION OF PROTECTION SYSTEM IN RCS MID-POINT GROUNDING CONFIGURATION

A. CONFIGURATION OF FAULT TESTS FOR VERIFICATION

In this study, fault tests were conducted to validate the adequacy of the protection system in a uni-polar LVDC system employing the proposed RCS mid-point grounding configuration. The fault test comprised an isolated converter, DC-RCD, IMD, load, etc., with the configuration and specifications detailed in Fig. 6 and Table 6.

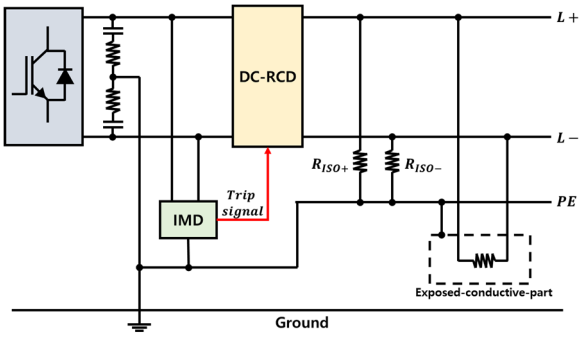

FIGURE 5. Proposed protection configuration for the uni-polar LVDC system with RCS mid-point grounding.

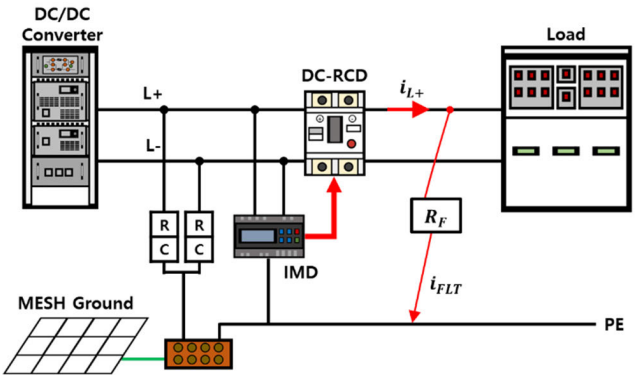

FIGURE 6. Test circuit for the verification of the protection system in a uni-polar LVDC system with RCS mid-point grounding configuration.

TABLE 6. Parameters of components for test circuit.

Component		Value
Isolated DC/DC Converter	Input	750 [Vdc]
	Output	380 [Vdc]
DC-RCD	Rated residual current	80 [mA]
	Operation time	100 [ms]
Load	76 [Ω]	
Fault resistor (R_F)	10, 285, 880 [Ω]	
	100 [kΩ]	
Grounding resistance	5 [Ω] or less	

Fault resistances used for simulating electric shocks ranged from the minimum to the maximum values of human body resistance (285 Ω, 880 Ω, as listed in Table 4. For ground fault and high-resistance faults, 10 Ω and 100 Ω were employed, respectively.

Table 7 presents the experimental conditions for the fault test aimed at validating the protection system in the RCS mid-point grounding configuration. Cases 1 to 4 assessed the operation of the DC-RCD while varying the RCS mid-point parameters, and Case 5 examined the functionality of IMD protection during high-resistance faults.

TABLE 7. Case parameters of the RCS mid-point grounding and fault resistor.

Case	RCS mid-point Grounding	Fault resistor (R_F)
1	RCS Mid-point (1870 [Ω] / 3 [μF])	10, 285, 880 [Ω]
2	RCS Mid-point (1870 [Ω] / 30 [μF])	10, 285, 880 [Ω]
3	RCS Mid-point (1870 [Ω] / 63 [μF])	10, 285, 880 [Ω]
4	RCS Mid-point (1870 [Ω] / 90 [μF])	10, 285, 880 [Ω]
5	RCS Mid-point (1870 [Ω] / 63 [μF]) RCS Mid-point (1870 [Ω] / 90 [μF])	100 [kΩ]

B. FAULT TEST RESULTS

Fig. 7 depicts the waveform of load current and fault current for Case 1. The peak fault current values during a fault, as shown in Fig. 7(b), are 245 mA, 145 mA, and 110 mA for each fault resistor, exceeding the rated residual current of the DC-RCD. However, the duration of the fault current exceeding 80 mA was less than 30 ms, which did not meet the time requirement for DC-RCD operation, as confirmed in Fig. 7(a). Consequently, the DC-RCD did not activate.

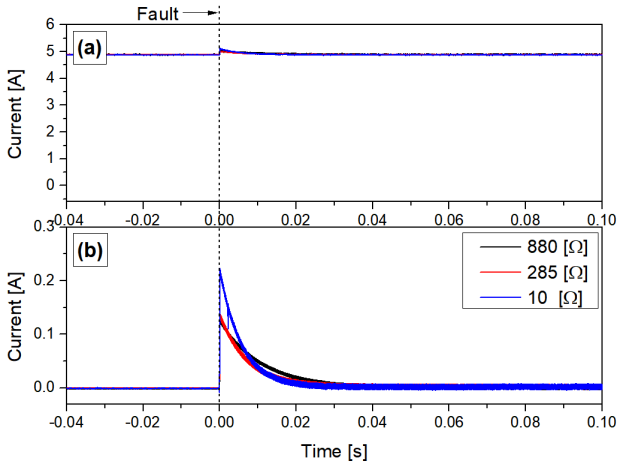

FIGURE 7. Experimental Waveform of Case 1 (a) Load current (i_{Load}), (b) fault current (i_{FLT}).

Fig. 8 shows the waveform of load current and fault current for Case 2. The peak fault current values during a fault, as demonstrated in Fig. 8(b), are 228 mA, 171 mA, and 109 mA for each fault resistor, once again exceeding the rated residual current of the DC-RCD. For cases utilizing fault resistances of 10 Ω and 285 Ω, the DC-RCD operated within 52 ms and 57 ms to disconnect the power, respectively. However, it did not operate for the 880 Ω fault, thereby failing to mitigate the risk of electric shock for the left foot to right foot path. In particular, a fault current exceeding 80 mA persisted for approximately 30 ms. Nevertheless, the duration necessary for DC-RCD operation was not sustained, resulting in no disconnection.

Fig. 9 shows the waveform of load current and fault current for Case 3. The peak fault current values during a fault, as shown in Figure 9(b), are 225 mA, 188 mA, and 124 mA for each fault resistor, exceeding the rated residual current of the DC-RCD. In all cases simulating ground faults and electric shocks, the DC-RCD operated within 53 ms, 54 ms, and 66 ms to disconnect the power.

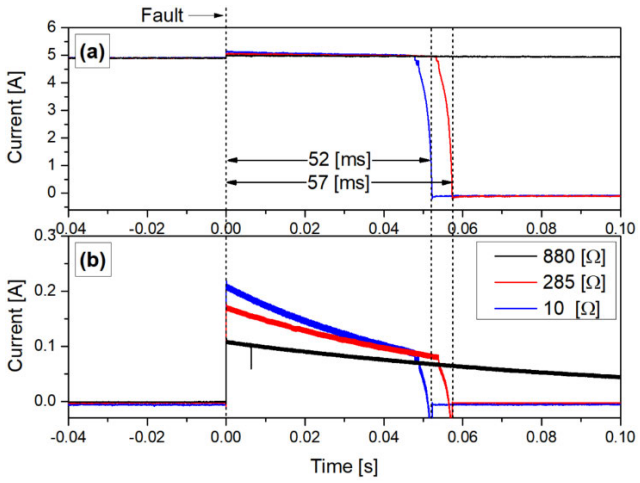

FIGURE 8. Experimental Waveform of Case 2 (a) Load current (i_{Load}), (b) fault current (i_{FLT}).

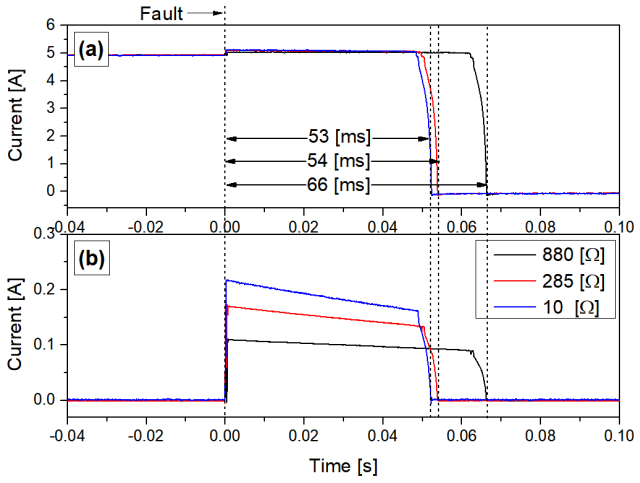

FIGURE 9. Experimental Waveform of Case 3 (a) Load current (i_{Load}), (b) fault current (i_{FLT}).

Based on the fault test results of Cases 2 and 3, where the LVDC system was effectively protected by the DC-RCD within 70 ms, it was affirmed that the proposed RCS mid-point grounding configuration with the appropriate parameters can be utilized in LVDC systems for protective operation without any power loss in the normal state.

Fig. 10 shows the waveform of load current and fault current for Case 4. The peak fault current values during a fault, as shown in Figure 10(b), are 217 mA, 182 mA, and 118 mA for each fault resistor, exceeding the rated residual current of the DC-RCD. In all cases simulating ground faults and electric shocks, the DC-RCD operated within 53 ms, 54 ms, and 63 ms to disconnect the power.

As evidenced in the fault test, the fault current exhibits a characteristic waveform akin to discharge current from capacitors. Hence, it is important to maintain the capacitor's condition because the proposed LVDC system cannot function if the capacitor fails due to deterioration, external surge inrush, opening and closing surge, etc.

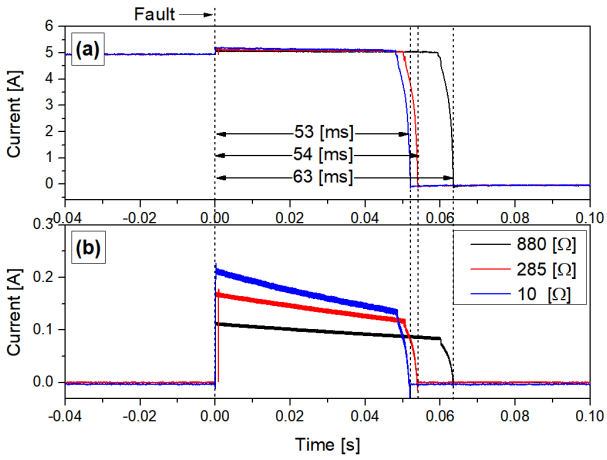

FIGURE 10. Experimental Waveform of Case 4 (a) Load current(i_{Load}), (b) fault current (i_{FLT}).

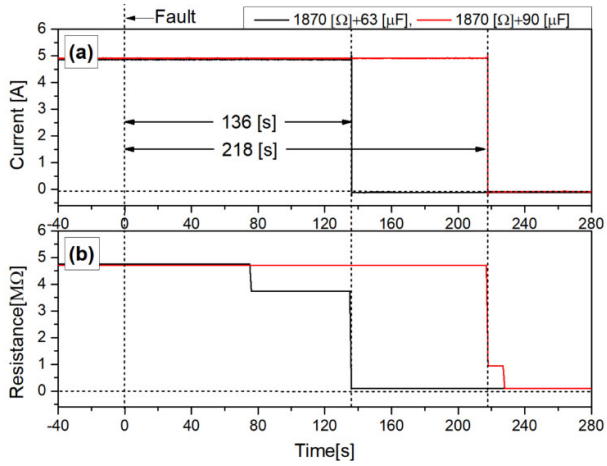

FIGURE 11. Experimental Waveform of Case 5 (a) Load current(i_{Load}), (b) Insulation resistance measured by IMD.

Even with capacitor values higher than those proposed in this study, it was verified that the fault current maintained the requisite operating time for DC-RCD operation in instances of ground faults and electric shocks. However, excessive capacitance can pose issues when IMD is applied, as it distorts the detection signal of IMD, even if the operation of the DC-RCD is normal.

Fig. 11 shows the load current and insulation of Case 5 during high-resistance faults. In Fig. 11(b), the insulation resistance measured using the IMD progressively decreases from approximately 4.7 Ω before the fault to approximately 10 Ω after the fault. In Fig. 11(a), the time required for the IMD to detect the fault leading to DC-RCD operation was 136 ms and 218 ms using a 63 μF and 90 μF capacitor, respectively, in the RCS mid-point grounding configuration. It was observed that as the capacitance increased, the detection time of the IMD extended by 82 ms. Thus, it was confirmed that excessive capacitance values elevate the risk by prolonging the fault detection time for secondary protection using IMDs, despite the advantage of high capacitance facilitating the operation of the DC-RCD.

VI. CONCLUSION

This study investigated the protection system of the RCS mid-point grounding configuration in uni-polar LVDC systems to ensure electrical safety. It evaluated the feasibility of protection systems in uni-polar LVDC systems with RCS mid-point grounding, utilizing DC-RCDs and IMDs for detecting electric shocks and ground faults. The analysis demonstrates that employing the RCS mid-point grounding configuration reduces the risk of inrush currents during initial energization and enables protection by DC-RCDs and IMDs, which are not available in other mid-point grounding configurations. To ensure the proper operation of protective devices, a scheme has been proposed for selecting mid-point earthing parameters. Thus, fault experiments were conducted, and the protective operation characteristics of DC-RCDs and IMDs based on parameter changes in the RCS mid-point grounding configuration were analyzed. As a result, it was found that DC-RCD detects impulsive fault current and operates within 80 ms. In cases of high-resistance faults undetectable by DC-RCDs, it was confirmed that faults can be detected and cleared within 4 minutes through the IMD.

The results indicate that protective coordination in uni-polar LVDC systems based on DC-RCDs and IMDs can be achieved through appropriate parameter selection.

Consequently, this study is deemed to contribute to establishing a safe uni-polar LVDC power system for end-users, mitigating electrical shock and system faults by proposing the RCS mid-point grounding system with protection methods. Additionally, it contributes to reducing construction costs by establishing a protection system based on relatively inexpensive mechanical circuit breakers instead of the high-cost semiconductor-based breakers used for consumer protection devices.

REFERENCES

[1] D. Siingh, R. P. Singh, N. J. Victor, and A. K. Kamra, "The DC and AC global electric circuits and climate," *Earth-Sci. Rev.*, vol. 244, Sep. 2023, Art. no. 104542, doi: 10.1016/j.earscirev.2023.104542.

[2] M. Delmotte. (2019). *Global Warming of 1.5 °C an IPCC Special Report on the Impacts of Global Warming*. [Online]. Available: www.environmentalgraphiti.org

[3] A. Jhunjhunwala, A. Lolla, and P. Kaur, "Solar-DC microgrid for Indian homes: A transforming power scenario," *IEEE Electrific. Mag.*, vol. 4, no. 2, pp. 10–19, Jun. 2016, doi: 10.1109/MELE.2016.2543950.

[4] Q. Ali, M. L. Di Silvestre, P. Lombardi, E. R. Sanseverino, and G. Zizzo, "The role of renewable energy generation in electric vehicles transition and decarbonization of transportation sector," in *Proc. IEEE Int. Conf. Environ. Electr. Eng. IEEE Ind. Commercial Power Syst. Eur.*, Madrid, Spain, Jun. 2023, pp. 1–6, doi: 10.1109/eeeic/icpseurope57605.2023.10194766.

[5] H. Wang, X. Jia, J. Li, X. Guo, B. Wang, and X. Wang, "New single-stage EV charger for V2H applications," in *Proc. IEEE 8th Int. Power Electron. Motion Control Conf.*, Hefei, China, May 2016, pp. 2699–2702.

[6] U. Boeke and M. Wendt. *Comparison of Low Voltage AC and DC Power Grids*. Accessed: 2024. [Online]. Available: https://www.upn.se/html-files/Glava/Referenser/Ref%201%20Boeke-Comparison_of_low_voltage_AC_and_DC_power_grids.pdf

[7] *Global DC Distribution Network Market*, Mordor Intell., Hyderabad, India, 2023.

[8] J. Rekola, A. Virtanen, J. Jokipii, and H. Tuusa, "Comparison of converter losses in an LVDC distribution," in *Proc. 38th Annu. Conf. IEEE Ind. Electron. Soc.*, Oct. 2012, pp. 1240–1245.

[9] S. S. Rath, G. Panda, P. K. Ray, and A. Mohanty, "A comprehensive review on microgrid protection: Issues and challenges," in *Proc. 3rd Int. Conf. Energy, Power Environ., Towards Clean Energy Technol.*, Meghalaya, India, Mar. 2021, pp. 1–6, doi: 10.1109/ICEPE50861.2021.9404520.
[10] K. Kant and O. H. Gupta, "DC microgrid: A comprehensive review on protection challenges and schemes," *IETE Tech. Rev.*, vol. 40, no. 4, pp. 574–590, Jul. 2023, doi: 10.1080/02564602.2022.2136271.
[11] L. Li, K.-J. Li, K. Sun, Z. Liu, and W.-J. Lee, "A comparative study on voltage level standard for DC residential power systems," *IEEE Trans. Ind. Appl.*, vol. 58, no. 2, pp. 1446–1455, Mar. 2022, doi: 10.1109/TIA.2021.3140161.
[12] S.-T. Lim, K.-Y. Lee, D.-J. Chae, C.-H. Oh, and S.-H. Lim, "Fault analysis of the mid-point grounding with capacitors in unipolar LVDC system," *J. Electr. Eng. Technol.*, pp. 1–8, Sep. 2023, doi: 10.1007/s42835-023-01642-5.
[13] T. Wang, A. Monti, R. Goldbeck, and R. W. De Doncker, "Voltage selection and personal safety in low voltage direct current networks at customer end," in *Proc. IEEE PES Innov. Smart Grid Technol. Conf. Eur.*, Sarajevo, Bosnia and Herzegovina, Oct. 2018, pp. 1–6, doi: 10.1109/ISGTEUROPE.2018.8571822.
[14] D.-W. Kim, Y.-B. Lim, S.-I. Lee, M.-I. Choi, and H.-W. Moon, "Protection techniques against electric shock in low voltage DC grounding systems depending on the analysis of earth fault current paths," *Trans. Korean Inst. Electr. Engineers*, vol. 65, no. 1, pp. 232–238, Jan. 2016, doi: 10.5370/kiee.2016.65.1.232.
[15] X. Kong, L. Li, J. Zhang, H. Wang, J. Zhou, G. Shi, and X. Cai, "Operation and control of DC solid state transformer with bipolar LVDC ports," in *Proc. IEEE 12th Energy Convers. Congr. Expo.*, Singapore, May 2021, pp. 402–407, doi: 10.1109/ECCE-Asia49820.2021.9479151.
[16] J. Liao, C. Guo, L. Zeng, W. Kang, N. Zhou, and Q. Wang, "Analysis of residual current in low-voltage bipolar DC system and improved residual current protection scheme," *IEEE Trans. Instrum. Meas.*, vol. 71, pp. 1–13, 2022, doi: 10.1109/TIM.2022.3200116.
[17] T. Kaipia, P. Salonen, J. Lassila, and J. Partanen, "Possibilities of the low voltage DC distribution systems," in *Proc. NORDAC Conf.*, Stockholm, Sweden, Aug. 2006, pp. 1–10.
[18] V. B. Subbaraj, "LVDC for buildings in The Netherlands: Technical and commercial potentials from DC office lab," M.S. thesis, Dept. Elect. Eng., Math. Comput. Sci., Delft Univ. Technol., Delft, The Netherlands, 2019.
[19] J. Mohammadi, F. B. Ajaei, and G. Stevens, "Grounding the DC microgrid," *IEEE Trans. Ind. Appl.*, vol. 55, no. 5, pp. 4490–4499, Sep. 2019, doi: 10.1109/TIA.2019.2928278.
[20] A. Makkieh, R. Pena-Alzola, A. Emhemed, G. Burt, and A. Junyent-Ferre, "Capacitive earthing charge-based method for locating faults within a DC microgrid," in *Proc. IEEE 3rd Int. Conf. DC Microgrids (ICDCM)*, Matsue, Japan, May 2019, pp. 1–6, doi: 10.1109/ICDCM45535.2019.9232921.
[21] X. Zhao, L. Chen, G. Li, J. Xu, and J. Yuan, "Coordination method for DC fault current suppression and clearance in DC grids," *CSEE J. Power Energy Syst.*, vol. 8, no. 5, pp. 1438–1447, Sep. 2022, doi: 10.17775/CSEEJPES.2019.03160.
[22] *Effects of Current on Human Beings and Livestock—Part 1: General Aspects*, Standard IEC 60479-1, 2018.
[23] *Effects of Current on Human Beings and Livestock—Part 2: Special Aspects*, Standard IEC 60479-2, 2019.
[24] S. Wang, H. Li, Q. Liu, W. Su, and C. Wang, "Research on the requirements for the break time of DC-RCD under different voltage levels and grounding modes in LVDC system," in *Proc. IEEE 4th Conf. Energy Internet Energy Syst. Integr. (EI)*, Wuhan, China, Oct. 2020, pp. 3675–3680, doi: 10.1109/EI250167.2020.9347386.
[25] I. Almutairy and J. Asumadu, "Examination of breaker-based protection systems for implementation in LVDC SSCB applications," in *Proc. IEEE 8th Annu. Comput. Commun. Workshop Conf. (CCWC)*, Las Vegas, NV, USA, Jan. 2018, pp. 509–514, doi: 10.1109/CCWC.2018.8301697.
[26] P. Aditya, S. N. Banavath, A. Lidozzi, A. Chub and D. Vinnikov, "Bidirectional sscb for residential dc microgrids with reduced voltage and current stress during fault interruption," in *Proc. IEEE 17th Int. Conf. Compat., Power Electron. Power Eng. (CPE-POWERENG)*, Tallinn, Estonia, 2023, pp. 1-6, doi: 10.1109/CPE-POWERENG58103.2023.10227379.
[27] S.-T. Lim, K.-Y. Lee, D.-W. Kim, D.-J. Chae, D.-S. Lim, and J.-H. Moon, "Selection of the earthing impedance at the source and electrical human effect in IT ground LVDC system for the end user's," *Trans. Korean Inst. Electr. Engineers*, vol. 70, no. 2, pp. 432–438, Feb. 2021, doi: 10.5370/kiee.2021.70.2.432.
[28] D. Cheng, B. Zhang, S. Xiong, Z. Xie, and Z. Xue, "Residual current detection prototype and simulation method in low voltage DC system," *IEEE Access*, vol. 10, pp. 51100–51109, 2022, doi: 10.1109/ACCESS.2022.3172698.
[29] A. Saxena, N. K. Sharma, and S. R. Samantaray, "An enhanced differential protection scheme for LVDC microgrid," *IEEE J. Emerg. Sel. Topics Power Electron.*, vol. 10, no. 2, pp. 2114–2125, Apr. 2022, doi: 10.1109/JESTPE.2022.3144300.
[30] *Low-Voltage Electrical Installations—Part 1: Fundamental Principles, Assessment of General Characteristics, Definitions*, Standard IEC 60364-1, 2009.
[31] S.-T. Lim, K.-Y. Lee, D.-J. Chae, and S.-H. Lim, "Design of mid-point ground with resistors and capacitors in mono-polar LVDC system," *Energies*, vol. 15, no. 22, p. 8653, Nov. 2022, doi: 10.3390/en15228653.

SEUNG-TAEK LIM was born in Seoul, Republic of Korea, in July 1992. He received the B.S., M.S., and Ph.D. degrees in electrical engineering from Soongsil University, Seoul, in 2016, 2018, and 2024, respectively. Since 2018, he has been a Senior Researcher with the Electrical Safety Research Institute, Korea Electrical Safety Corporation (KESCO).

KI-YEON LEE was born in Seoul, Republic of Korea, in May 1975. He received the B.S. and M.S. degrees in electrical engineering from Incheon National University, Incheon, South Korea, in 2002 and 2004, respectively, and the Ph.D. degree in IT applied system engineering from Jeonbuk National University, Jeollabuk-do, South Korea, in 2020. Since 2004, he has been the Head Researcher of the Electrical Safety Research Institute, Korea Electrical Safety Corporation (KESCO).

DONG-JU CHAE was born in Gwangju, Republic of Korea, in July 1981. He received the B.S. and M.S. degrees in electrical engineering from Korea University, Seoul, South Korea, in 2008 and 2011, respectively. Since 2014, he has been a Senior Researcher with the Electrical Safety Research Institute, Korea Electrical Safety Corporation (KESCO).

CHAN-HYEOK OH was born in Gwangju, Republic of Korea, in May 1988. He received the B.S., M.S., and Ph.D. degrees in electrical engineering from Chonnam National University, Gwangju, in 2015, 2017, and 2022, respectively. Since 2022, he has been a Senior Researcher with the Electrical Safety Research Institute, Korea Electrical Safety Corporation (KESCO).

SUNG-HUN LIM was born in Jeonju, Republic of Korea, in November 1973. He received the B.S., M.S., and Ph.D. degrees from Jeonbuk National University, Jeollabuk-do, South Korea, in 1996, 1998, and 2003, respectively. Since 2006, he has been a Professor with the Department of Electrical Engineering, Soongsil University, Seoul, South Korea.